Materials Research Bulletin 150 (2022) 111758

Contents lists available at ScienceDirect

Materials Research Bulletin

journal homepage: www.elsevier.com/locate/matresbu

Research Papers

Magnetic and magnetocaloric properties of nanocrystalline sample of a glassy ferromagnetic compound: Modification of short range ordering

Soma Chatterjee [a], Dipak Mazumdar [a], Kalipada Das [b,*], I. Das [a]

[a] CMP Division, Saha Institute of Nuclear Physics, HBNI, AF-Bidhannagar, Kolakta-700064, India
[b] Department of physics, Seth Anandram Jaipuria College, 10-Raja Nabakrishna Street, Kolkata-700005, India

ARTICLE INFO

PACS numbers:
75.47.Lx
73.63.Bd

Keywords:
Manganites
Magnetocaloric effect
Nanocrystalline compound

ABSTRACT

The modification of magnetic interactions due to the reduction of particle size has been explored in the case of nanocrystalline $Gd_{0.5}Sr_{0.5}MnO_3$ compound. In contrast to the normal ferromagnetic or antiferromagnetic compounds, the studied nanoparticle exhibits quite different magnetic and magnetocaloric properties. The experimental outcomes are also compared with its bulk counterparts having disordered ferromagnetic ground state. Additionally, at the cryogenic temperature range, the significant magnetocaloric effect in both the samples indicate the applicability as a suitable magnetic refrigerant material. Moreover, the desertion nature of the magnetic hysteresis loop due to the field cycling indicates the superiority of the nanocrystalline compound over its bulk counterpart.

1. Introduction

Doped perovskite manganites having the general formula $R_{1-x}B_xMnO_3$ (R = trivalent ion, B= bivalent ion) have received utmost attention due to their several fundamental and beneficial aspects [1,2]. The striking correlation between several degrees of freedom populates different rich physical properties. Generally, undoped manganites exhibit antiferromagnetic-insulating ground state [3]. However, doping with a bivalent ion at the trivalent site produces Mn^{4+} ions whose physical properties are drastically modified [4–6]. Doping-induced intriguing properties like metal-insulator transition, charge-ordering, colossal magnetoresistance, ferromagnetism, etc. have been noticed in the doped manganite systems [7,8]. Charge ordering is the real space ordering of Mn^{3+} and Mn^{4+} ions in a crystal, which is almost a generic phenomenon in doped perovskite manganites near the half-doped region. In most of the cases, below the charge ordering transition temperature, doped perovskite manganites exhibit antiferromagnetic-insulating ground state [6]. It should be mentioned that there is a strong correlation between magnetic and electrical properties of the doped perovskite manganite systems [7,8]. In the case of the antiferromagnetic ground state, insulating nature is dominant in nature [9], while ferromagnetism favors the metallic ground state [10]. However, a different scenario is also reported in the case of several manganite compounds [11,12]. More specifically, compounds having no long-range magnetic ordering (unlike glassy magnetic state), sometimes they exhibit a comparatively large value of magnetization with electrically insulating ground state [13].

For some doped perovskite compound, the physical properties are very much sensitive to its dimensions [14,15]. In the case of nanoparticles, the surface effect plays an important role to determine their physical properties. Several experimental outcomes are strongly modified due to the reduction of the particle size. It is already reported that the reduction of particle size may cause different nature of the magnetic ground state. Previous studies indicate that for the antiferromagnetic bulk compounds, a phase-separated (ferromagnetic and antiferromagnetic) core-shell type structure stabilizes in its nanocrystalline form [16]. Similarly, an opposite behavior has also been reported for the ferromagnetic compounds [17]. During the last two decades, the modification of the physical properties of the nanoparticles for ferromagnetic and antiferromagnetic compounds was extensively studied. However, less attention has been paid to studying the modification of the physical properties of the nanoparticles of a glassy magnetic system.

In context to the magnetocaloric effect, apart from several beneficial aspects, due to the higher production cost of intermetallic materials, scientists have focused their attention towards the alternating sources of refrigerant materials having low cost production values. Doped perovskite manganites are greatly attractive due to their several beneficial aspects [1,2]. Besides this fundamental importance, another great aspect

* Corresponding author.
E-mail address: kalipadadasphysics@gmail.com (K. Das).

https://doi.org/10.1016/j.materresbull.2022.111758
Received 9 November 2021; Received in revised form 16 January 2022; Accepted 17 January 2022
Available online 19 January 2022

Table 1
Lattice parameters of GSMO-bulk and GSMO-nanocrystalline compounds

Compound	Space group	a (Å)	b (Å)	c (Å)
GSMO-bulk	Pnma	5.4588	5.4150	7.6464
GSMO-nanocrystalline	Pnma	5.4169	5.3929	7.6909

of the magnetocaloric effect is related to the selection of magnetic refrigerant materials. Generally, the materials having a large magnetocaloric effect may be selected as a potential candidate for magnetic refrigeration purposes [18–21]. However, for a good refrigerant material with a large magnetocaloric effect, some other physical properties (insulating nature, hysteresis loss, working temperature range, etc.) should also be checked.

Among the disorder/glassy magnetic system, $Gd_{1-x}Sr_xMnO_3$ is one of the most well-studied compound [22–24]. Specifically, for $x = 0.5$, there are several reports where the magneto-transport and magnetic properties were well-addressed [22,23]. Wagh et al. had reported the insulating nature (glassy magnetic state) of the $Gd_{0.5}Sr_{0.5}MnO_3$ compound in the presence of $H < 80$ kOe magnetic field [24]. Beyond this field value ($H > 80$ kOe), the glassy magnetic state was transformed into a ferromagnetic state and exhibited a metal-insulator transition [24]. According to the previous study, it is quite clear that the short-range interaction is modified in the presence of different external magnetic fields. As the magnetocaloric effect is directly correlated with the suppression of the magnetic randomness to the external magnetic field, a significant magnetocaloric effect may be expected for this compound.

Our experimental outcomes indicate significantly large magnetocaloric effect at the cryogenic temperature range in the case of the bulk GSMO compound. Modification of magnetic ground state is observed on application of the external magnetic field, a However, due to the field-induced melting of the charge-ordered fractions, a prominent hysteresis is present in the bulk form. In contrast to that, in the case of the nanocrystalline compound, superparamagnetic nature is found without any field-dependent hysteresis loop. In addition to that, the estimated value of magnetic entropy change in the nanocrystalline compound is comparable to its bulk form, which is beneficial from the technological perspective.

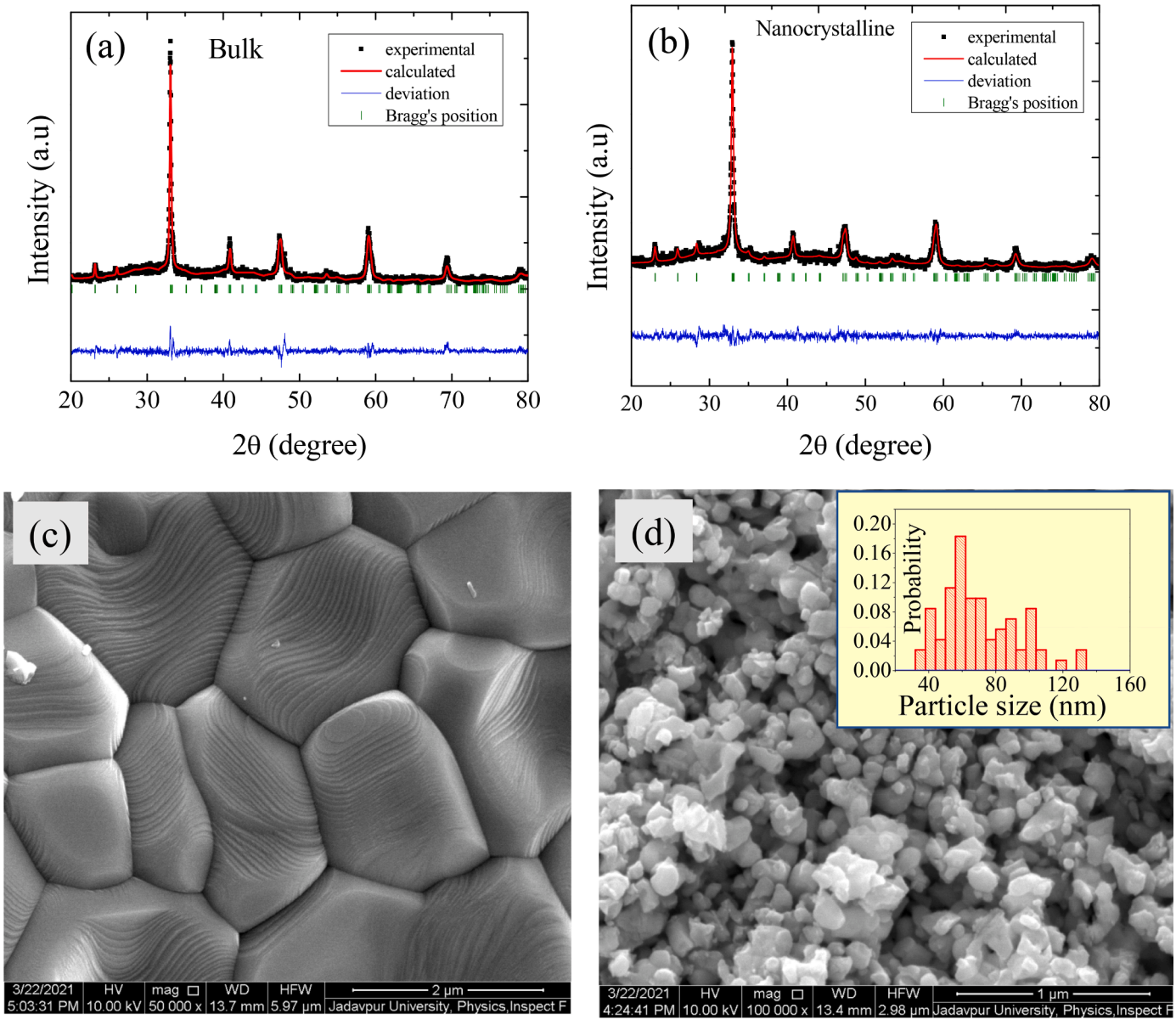

Fig. 1. Room temperature x-ray diffraction pattern (along with profile fitting) for (a) bulk and (b) nanocrystalline compound. (c) and (d) represents the scanning electron microscopy images of bulk and nanocrystalline compound respectively. The particle size distribution of the nanocrystalline sample is given in the inset of (d).

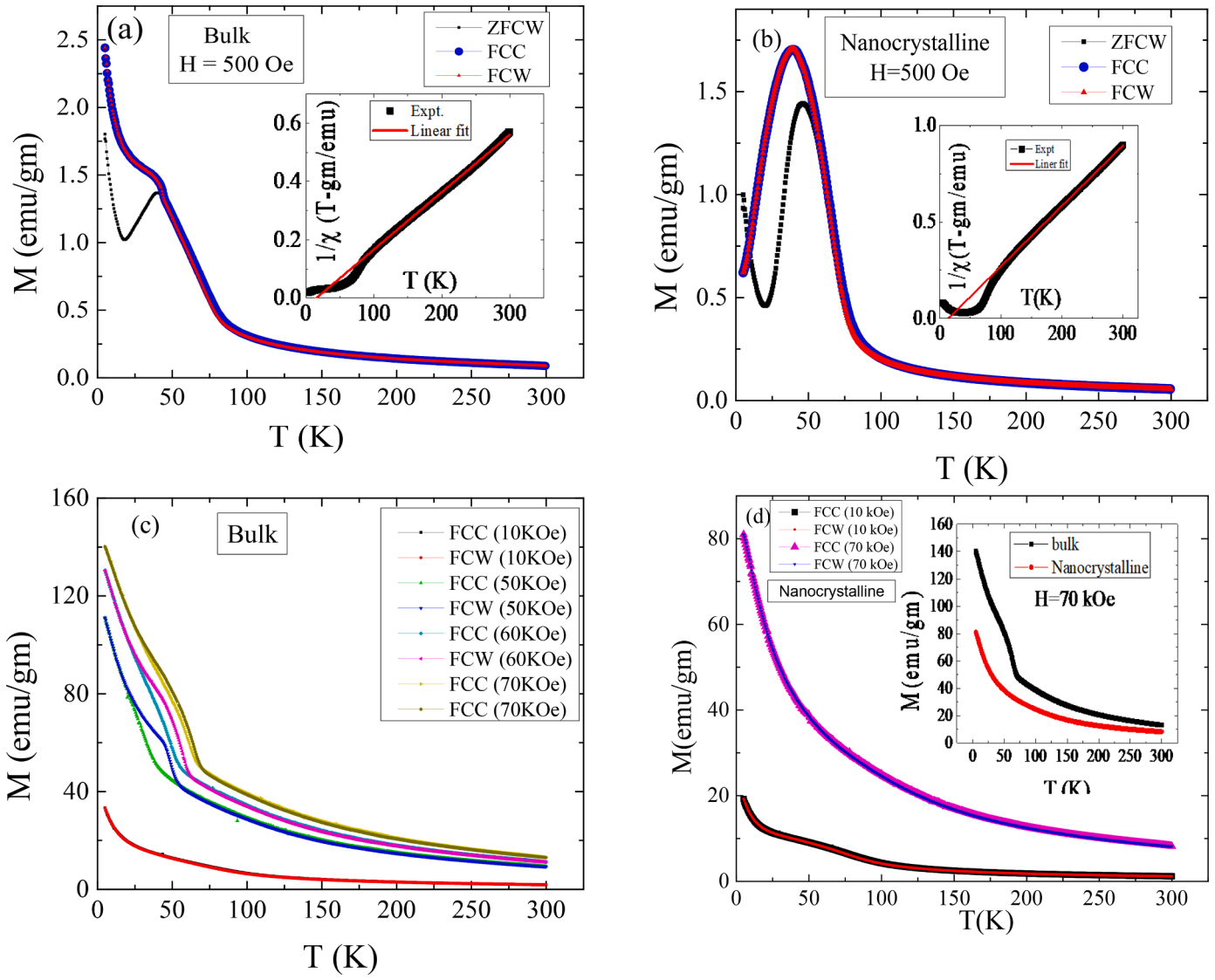

Fig. 2. Temperature dependence of ZFCW, FCW, FCC magnetization at H = 500 Oe (a) for Bulk and (b) for nanocrystalline $Gd_{0.5}Sr_{0.5}MnO_3$ compound respectively. Insets show the temperature dependence of inverse susceptibility (calculated from FCW magnetization). The nature of magnetization as a function of temperature at higher magnetic fields are shown in (c) for bulk compound and (d) for nanocrystalline compound. The inset of (d) indicates the qualitative nature of the M(T) for bulk and nanocrystalline compound at H = 70 kOe external magnetic field.

2. Sample preparation, characterizations and measurements

The $Gd_{0.5}Sr_{0.5}MnO_3$ (GSMO) compounds were prepared by well known sol-gel method. The starting materials were highly pure (99.99 %) Gd_2O_3 (pre-heated), $SrCO_3$, and MnO_2. For the preparation of clear individual polycrystalline bulk and nanocrystalline water solutions, a suitable amount of concentrated nitric acid and millipore water were added with all the initial components. In the case of MnO_2, an appropriate amount of oxalic acid was given due to its insolubility nature in nitric acid. Finally, all the individual solutions were homogeneously mixed-up with a magnetic stirrer and a suitable amount of citric acid was added. The mixed solution was slowly evaporated at 80-90 °C until the gel was formed by using a water bath. After the formation of gel, it was decomposed at a slightly higher temperature and black porous powder was observed. Finally, pelletized powder sample was annealed at 1300 °C for 36 hours for the preparation of the bulk compound and at 900 °C for 3 hours to prepare the nanocrystalline compound. The phase purity of the prepared samples was checked by the x-ray diffraction (XRD) measurement at room temperature using a Rigaku-TTRAX-III diffractometer, M/s Rigaku, Japan. For further characterization, a field emission scanning electron microscopy (FESEM) measurement was performed. A superconducting quantum interference device based on a vibrating sample magnetometer (SQUID-VSM) from Quantum Design, USA has been utilized to measure the magnetic properties and magnetocaloric effect for both the samples.

3. Results and discussion

The room temperature XRD measurements for the bulk and nanocrystalline sample indicate the chemically single-phase nature of the compounds. The Rietveld refinement (only profile fitting) was performed using 'Pnma' space group symmetry as reported in earlier study [23]. The estimated lattice parameters for GSMO-bulk and GSMO-nanocrystalline compounds are presented in Table 1. The experimental XRD data along with the profile fitted curves for the GSMO-bulk and GSMO-nanocrystalline compounds are presented in Fig. 1 (a) and (b) respectively.

We have also estimated the average crystalline size of the nanoparticles by using Scherrer's formula which is given below,

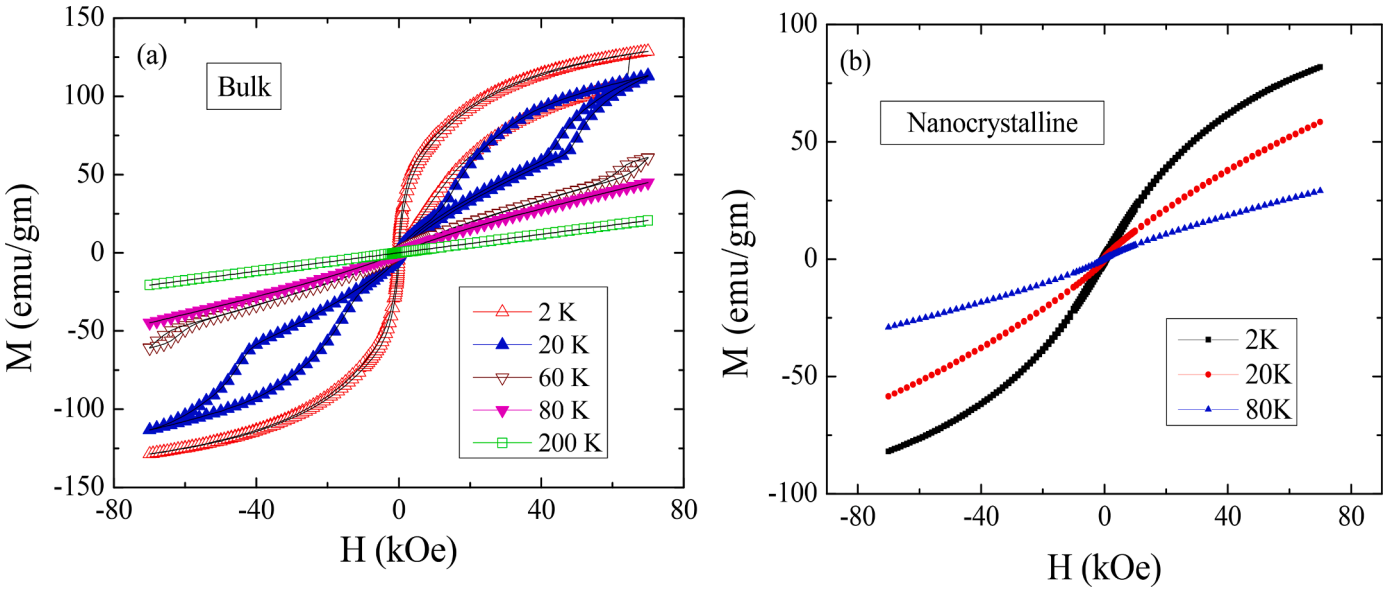

Fig. 3. (a) and (b) represents the magnetization as a function of the external magnetic field at some selected temperature for bulk and nanocrystalline compound respectively.

$$d = \frac{k\lambda}{\beta cos\theta} \tag{1}$$

where k ~ 0.94 (constant) and λ = 1.54 Å is the wavelength of the Cu-K_α radiation. In Eq. (1), β is the effective full-width at half-maxima (FWHM) for the predominant Bragg's peak of the nanocrystalline compound. This is estimated by the relation

$$\beta = B - \frac{b^2}{B} \tag{2}$$

where 'b' and 'B' are FWHM of a peak for bulk and nanocrystalline compounds respectively (measured by the same instrument). The estimated average particle size for the nanocrystalline compound was found to be ~ 56 nm. The scanning electron microscopy images for the bulk and nanocrystalline compounds are shown in Fig. 1 (c) and (d) respectively. The estimated average particle size of the nanocrystalline sample is comparable with the previous one as estimated from the x-ray line-width broadening.

Temperature dependence of the magnetization was measured in three different protocols which are described as follows:

Zero field cooled warming (ZFCW): To measure the magnetization in this protocol, the sample was first cooled down in the absence of any external magnetic field. At the lowest possible temperature (5 K in this case), the desired magnetic field was applied and the sample was warmed (rate 5 K/min). During the warming process, the temperature dependence of magnetization data was collected.

Field cooled cooling (FCC): In this protocol, a desired magnetic field was applied at room temperature and the temperature-dependent magnetization was recorded during cooling.

Field cooled warming (FCW): After cooling down the sample in the presence of a fixed magnetic field, the sample was again warmed with the same magnetic field and the magnetization as a function of temperature data was recorded.

The magnetization as a function of temperature in different external magnetic fields for the polycrystalline bulk and the nanocrystalline GSMO compounds are displayed in Fig. 2. In the case of bulk counterpart, a prominent bifurcation between ZFCW and FCC/FCW magnetization data has been observed at H =500 Oe external magnetic field (Fig. 2(a)). Additionally, below T = 100 K, there is a kink in the magnetization plot which manifests the presence of charge ordering signature of the compound as reported previously [23]. Wagh et al. had reported that at T = 42 K, a signature of a glassy magnetic state is present in this compound [23]. In our present study, such a signature is also found near the same temperature region. Magnetization responses in the presence of different higher magnetic field values are given in Fig. 2 (c). One important point should be mentioned that there is no thermal hysteresis in between the FCC and FCW data even at H = 10 kOe. However, a prominent splitting between FCC and FCW data (T<50 K) has appeared in the presence of higher field values (Fig. 2(c)). Such hysteretic nature at high field values may be associated with the signature of a field-induced transformation of the charge-ordered antiferromagnetic fraction into a ferromagnetic state. In contrast to that, at a lower magnetic field (H = 500 Oe), the magnetization of the nanocrystalline compound depicts a peak at the low-temperature region (Fig. 2 (b)). This implies the presence of a weak antiferromagnetic-type of magnetic ordering. A bifurcation between ZFCW and FCC/FCW curves has also appeared in the case of the bulk counterpart. Most interestingly, the splitting between the FCC and FCW magnetization measured in higher fields is totally absent in the nanocrystalline compound which is shown in Fig. 2(d).

To calculate the effective magnetic moment (P_{eff}), magnetic susceptibility data at high temperature is analyzed by using the well known Curie-Weiss law in the form of

$$\chi = \frac{C}{T - \theta} \tag{3}$$

where C is the Curie constant and θ is the paramagnetic Curie temperature. Considering all the moments for Mn^{3+}, Mn^{4+}, and Gd^{3+}, the calculated value of P_{eff} for $Gd_{0.5}Sr_{0.5}MnO_3$ compound is 7.142, while the experimental value of P_{eff} for the bulk and nanocrystalline compounds are 9.134 and 7.566 respectively. The higher experimental values of P_{eff} indicate the presence of ferromagnetic clusters in the paramagnetic region. The value of P_{eff} also decreases with decreasing the particle size which reflects the reduction of ferromagnetic cluster size [25].

To compare the qualitative nature of the magnetization of bulk and nanocrystalline compounds, the temperature dependent magnetization for both samples (H = 70 kOe) is shown in the inset of Fig. 2(d). The variation of the magnetization indicates that with increasing temperature, magnetization is more rapidly decreased for the nanocrystalline compound. Such nature might be associated with the reduction of the interaction strength (spin correlation) for decreasing the particle size as reported in an earlier study [26].

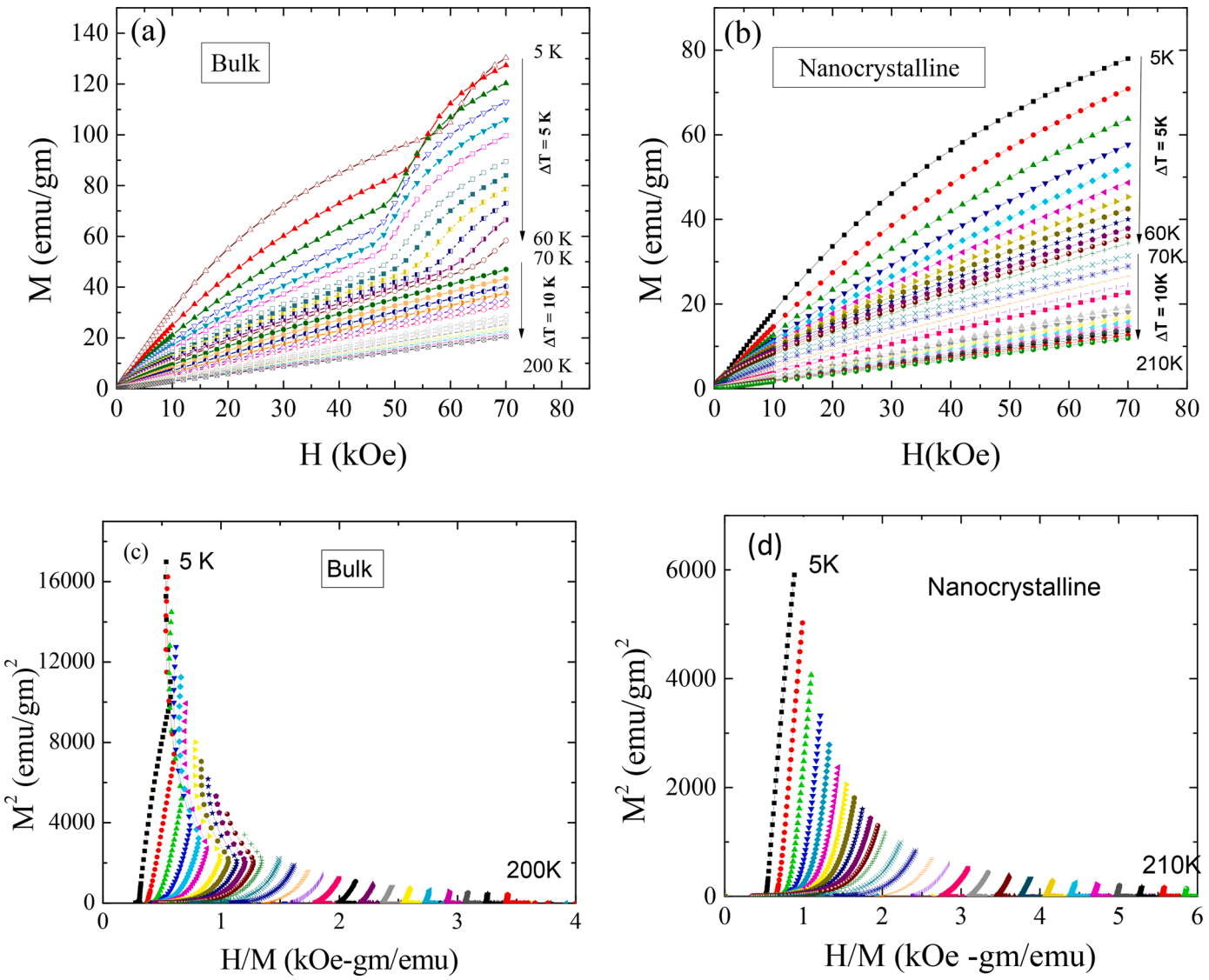

Fig. 4. One quadrant magnetization as a function of magnetic field for (a) Bulk and (b) nanocrystalline GSMO. (c)and (d) represents the M^2 vs. H/M plot of magnetic isotherms for bulk and nanocrystalline compound respectively and For 5-60 K temperature interval was 5 K and for 70-200 K, temperature interval was 10 K.

Magnetic field-induced splitting in the bulk sample (hysteresis) is more clearly notified in the field-dependent magnetization measurement. Isothermal magnetization of polycrystalline bulk and nanocrystalline samples were measured at different constant temperatures. For recording the field-dependent magnetization data, the sample was first cooled down from its paramagnetic region in the absence of any external magnetic field. After reaching the desired temperature, the magnetic field was applied and the corresponding magnetization value was recorded. For the sake of clarity, isothermal magnetization data for some selected temperatures are shown in Fig. 3. The pronounced hysteresis for the bulk sample indicates the phase separation nature at low temperature regions. Due to the application of an external magnetic field, charge-ordered antiferromagnetic phase fraction is transformed into a ferromagnetic one via a metamagnetic type transition. Such phase transformation results in a prominent hysteresis loop in the M-H measurement (Fig. 3 (a)). In contrast to that, the nanocrystalline sample exhibits quite different nature in the field-dependent magnetization measurement. Both the field-induced meta-magnetic type transition and hysteresis loop disappeared in the nanocrystalline compound (Fig. 3(b)). Such nature again indicates the reduction of the interaction (spin correlation) in the nanocrystalline compound.

It is well documented that MCE can be treated as a powerful tool to understand the different nature of the magnetic ground state [18]. In the present study, the ground state of the bulk sample is a glassy type phase separated in nature. However, due to the application of an external magnetic field, the ground state of the compound is modified and the field-induced ferromagnetic property becomes prominent. On the other hand, it is also reported that the suppression of the hysteresis loss is beneficial for magnetic refrigeration purpose [27]. Interestingly, magnetic measurement indicates that the hysteresis nature and magnetic interaction are drastically reduced in the nanocrystalline GSMO system. Considering these facts, we have studied the MCE properties for bulk as well as nanocrystalline compounds. To calculate the magnetocaloric entropy change, isothermal magnetization data were recorded for both samples. The isothermal magnetization as a function of magnetic field for bulk and nanocrystalline samples are shown in Fig. 4(a) and 4(b) respectively. According to Bannerjee's criterion, one can easily determine the order of phase transition from the slope of the Arrott plots (M^2 vs. H/M) [28]. Generally, for a second-order phase transition, the slopes of the Arrott plots should be positive whereas the negative slope implies the first-order phase transition. In our present study, the negative slopes indicate the dominant first-order nature of the transition in the bulk counterparts (Fig. 4(c)). However, in the nanocrystalline compound, such a clear signature of phase transition is absent (Fig. 4(d)). Magnetic

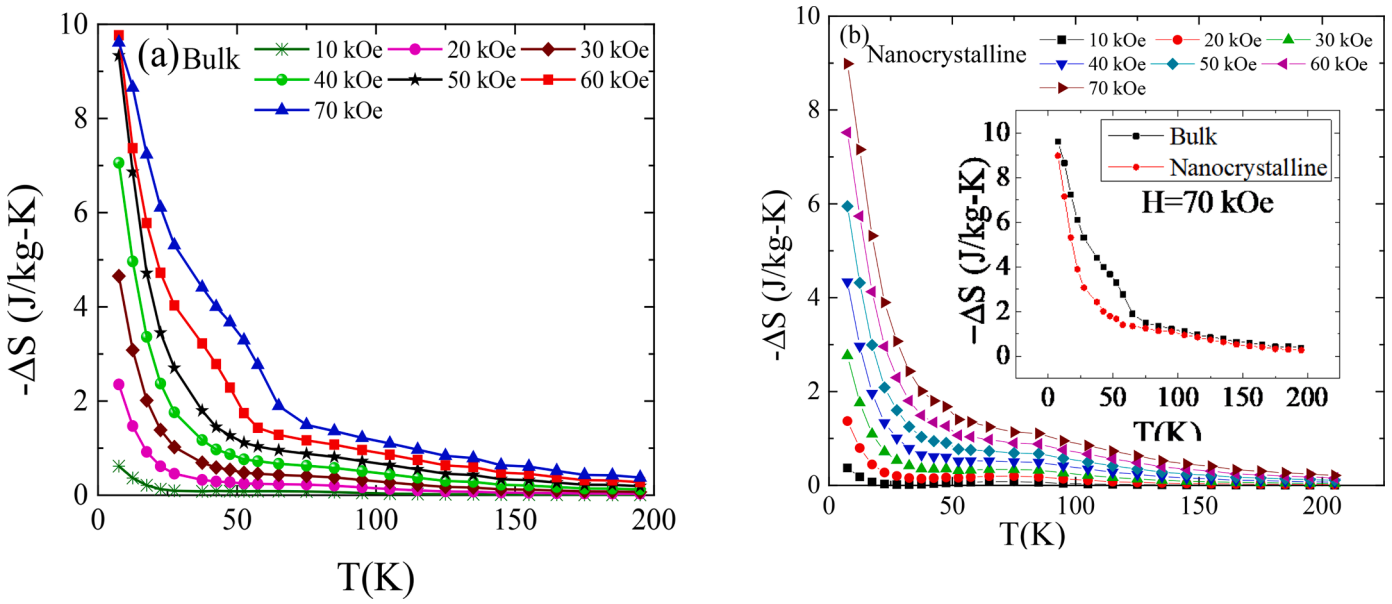

Fig. 5. Magnetocaloric entropy change as a function of temperature at the different external magnetic fields for (a) Bulk (b) Nanocrystalline $Gd_{0.5}Sr_{0.5}MnO_3$ compounds. Inset of (b) indicates the qualitative nature and quantitative comparison of MCE response of the bulk and nanocrystalline compound at H = 70 kOe external magnetic field.

entropy change is calculated by using Maxwell's thermodynamic relation which is given below,

$$\Delta S = \int_0^H \frac{\partial M}{\partial T} dH \tag{4}$$

The variation of the magnetic entropy change as the function of temperature at the different constant magnetic fields is given in Fig. 5. The magnetocaloric effect of the polycrystalline bulk sample is significantly large at the low-temperature region (cryogenic temperature range). Similar to the bulk counterpart, the highest magnetocaloric entropy change at the cryogenic temperature region is also appeared for the nanocrystalline compound. As mentioned earlier, materials exhibiting a large magnetocaloric effect at the cryogenic temperature range might be a potential candidate for the use of magnetic refrigerant material. Additionally, for the studied nanocrystalline compound, there is no hysteretic nature in the magnetization (Fig. 3(b)) due to the magnetic field cycling.

To concentrate on the quantitative value of magnetocaloric entropy change, it is well documented that for a ferromagnetic (antiferromagnetic) compound, the magnetocaloric effect (inverse magnetocaloric effect) is drastically reduced with the reduction of particle sizes [17,29]. In contrast to that, in our present study, the value of the maximum entropy change of the nanocrystalline sample is comparable to its bulk counterpart. Such interesting behavior of nanocrystalline compounds may be connected with the modification of the magnetic interaction and magnetic states.

To get more insights regarding the magnetic state of the nanocrystalline compound, Dong et al. had reported a detailed calculation considering the energy minimization concept [16]. According to their numerical simulation result, a spontaneous phase separation scenario may be stable in the case of nanocrystalline compound [16]. Moreover, there are some limiting cases where a stable superparamagnetic state may appear in the nanoparticles. Previously it was mentioned that for a superparamagnetic state, the M-H isotherms should follow the modified Langevin function [30]. In our present study, we have fitted the M-H isotherms considering the modified Langevin function which is given below,

$$M(H) = N\mu L\left(\frac{\mu H}{K_B T}\right) + \chi H \tag{5}$$

where N is the number density of cluster, μ is the average moment of each cluster [30], K_B is the Boltzmann constant, and L(x) is the standard Langevin function given as L(x) = (coth(x)-1/x). Here, the 'χH' term

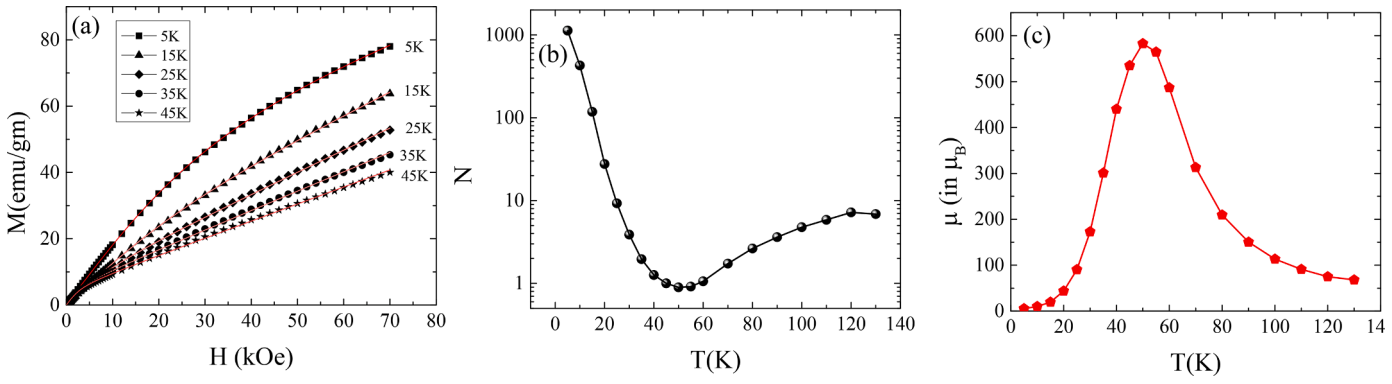

Fig. 6. (a) represents the fitting of some magnetic isotherms of Fig. 4 using the modified Langevin function given in Eq. (5). (b) and (c) represents the number density 'N' of the superparamagnetic (SPM) cluster and average moment of the clusters 'μ' as a function of temperature respectively.

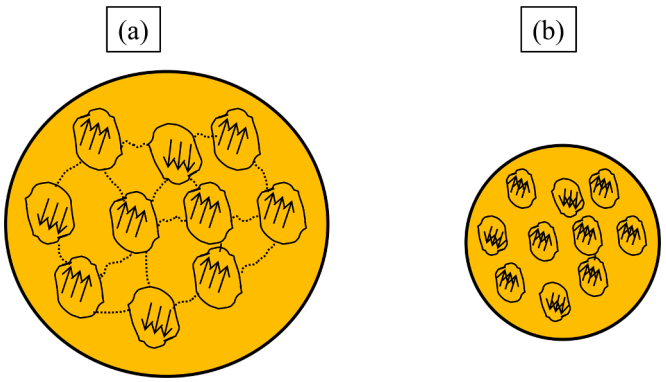

Fig. 7. Schematic representation of the magnetic state of (a) bulk and (b) nanocrystalline $Gd_{0.5}Sr_{0.5}MnO_3$ compound.

includes all the possible sources of linear magnetization with respect to the magnetic field. A good fitting was observed for the M-H curves by using Eq. (5). For the sake of clarity, some selected magnetic isotherms (for nanocrystalline sample) along with the fitted lines are shown in Fig. 6. From the fitting, we have extracted the parameters N and μ. The temperature dependence of N and μ are also plotted in Fig. 6. The variation of 'N' indicates a shallow minimum at T ~ 50 K, and μ depicts a maximum at the vicinity of the same temperature. Such nature may be addressed by considering the transformation of the small antiferromagnetic phase fractions (as mentioned in Fig. 2(b)) to a superparamagnetic one, even in the nanocrystalline compound. Generally, with increasing temperature, both 'N' and 'μ' parameters should be reduced [30]. However, in our present study, μ value is enhanced up to 50 K and then it decreases as usual. This experimental outcomes indicate a finite possibility of the existence of mixed magnetic phases (a small antiferromagnetic fraction with a superparamagnetic phase). Similarly, after a particular temperature (T ~ 50 K), the transformation of the antiferromagnetic counterpart into the superparamagnetic phase influences the variation of N.

There are numerous reports found in the literature regarding the modification of the surface-mediated physical properties in the nanocrystalline compound compared to their bulk counterparts [14,16,17]. For the antiferromagnetic bulk compound, the surface-induced phase--separated (ferromagnetic and antiferromagnetic) stable magnetic state appears in the case of the nanocrystalline form [16]. Similarly, for the nanoparticles of the ferromagnetic compound, an opposite nature was also observed in between the magnetic properties of the core and shell part (also mentioned in the introduction section) [17]. In contrast to that, our present study highlights the change of physical properties due to the reduction of the particle size for a disordered-glassy ferromagnetic compound. Magnetic and magnetocaloric effect studies indicate the co-existence of the superparamagnetic and small antiferromagnetic phase at the low-temperature region of the nanocrystalline compound.

Our concerned experimental outcomes, as well as discussions, indicate that for the bulk GSMO compound, the disordered ferromagnetic domains are magnetically interacting. However, due to the reduction of the particle size, magnetic interaction became feeble, and a superparamagnetic ground state has appeared. For better understanding, a very simple representation of the magnetic state for the bulk and nanocrystalline compounds is schematically shown in Fig. 7. Such reduction of the magnetic interaction in the nanoparticles was also earlier reported from the theoretical and experimental point of view [16, 26]. Regarding this context, as depicted in the insets of Figs. 2(d) and 5 (b), the quick reduction of the magnetization and magnetic entropy change (with temperature) of the nanocrystalline compound can be addressed considering such non-interacting nature of the magnetic domains.

4. Conclusions

To summarize, a comparative study of the magnetic and magnetocaloric effect of polycrystalline and nanocrystalline GSMO compounds is presented. Due to the reduction of the particle size, the ground state of the nanocrystalline compound is markedly modified in contrast to its bulk counterpart. As the magnetocaloric effect of both compounds is significantly large at the cryogenic temperature range, it may be considered as a magnetic refrigerant material. Additionally, the superiority of the nanocrystalline sample due to no hysteresis loss is addressed. The distinct nature of magnetization of the nanocrystalline compound (compared to bulk) is analyzed considering the formation of superparamagnetic nanoclusters.

Declaration of competing interest

All authors have participated in (a) conception and design, or analysis and interpretation of the data; (b) drafting the article or revising it critically for important intellectual content; and (c) approval of the final version.

Acknowledgment

The work was supported by Department of Atomic Energy (DAE), Govt. of India. Department of Physics, Jadavpur University is acknowledged for FESEM measurement and thanks to A. Karikar, S. Baradia for fruitful discussion.

References

[1] A. Biswas, T. Samanta, S. Banerjee, I. Das, J. Appl. Phys. 103 (2008), 013912.
[2] A. Biswas, S. Chandra, T. Samanta, M.H. Phan, I. Das, H. Srikanth, J. Appl. Phys. 113 (2013) 17A902.
[3] H.B. Hamed, M. Hoffmann, W.A. Adeagbo, A. Ernst, W. Hergert, Phys. Status Solidi B 257 (2020), 1900632.
[4] A.A. Wagh, K.G. Suresh, P.S. Anil Kumar, Suja Elizabeth, J. Phys. D: Appl. Phys. 48 (2015), 135001.
[5] T. Kimura, G Lawes, T Goto, Y Tokura, A.P. Ramirez, Phys. Rev. B 71 (2005), 224425.
[6] J.L. Cohn, M. Peterca, J.J. Neumeier, Phys. Rev. B 70 (2004), 214433.
[7] N.S. Bingham, P. Lampen, M.H. Phan, T.D. Hoang, H.D. Chinh, C.L. Zhang, S. W. Cheong, H. Srikanth, Phys. Rev. B 86 (2012), 064420.
[8] P. Lampen, N.S. Bingham, M.H. Phan, H. Kim, M. Osofsky, A. Pique, T.L. Phan, S. C. Yu, H. Srikanth, Appl. Phys. Lett. 102 (2013), 062414.
[9] Sun-Woo Kim, Chen Liu, Hyun-Jung Kim, Jun-Ho Lee, Yongxin Yao, Kai-Ming Ho, Jun-Hyung, Physical Review Letters 115 (2015) 9.
[10] T. Hotta, Phys. Rev. B 67 (2003), 104428.
[11] Sanjukta Paul, Sudhakar Yarlagadda, Phys. Rev. B 103 (2021), 035140.
[12] P.A. Algarabel, J.M. De Teresa, J. Blasco, M.R. Ibarra, Cz. Kapusta, M. Sikora, D. Zajac, P.C. Riedi, C. Ritter, Phys. Rev. B 67 (2003), 134402.
[13] A.K Kundu, P. Nordblad, C.N.R. Rao, J. Phys.: Condens. Matter 18 (2006) 4809–4818.
[14] S. Dong, R. Yu, S. Yunoki, J.-M. Liu, E. Dagotto, Phys. Rev. B 78 (2008), 064414.
[15] J.B. Goodenough, Phys. Rev. 100 (1955) 564.
[16] S. Dong, F. Gao, Z.Q. Wang, J.M. Liu, Z.F. Ren, Appl. Phys. Lett. 90 (2007), 082508.
[17] A. Rostamnejadi, M. Venkatesan, J. Alaria, M. Boese, P. Kameli, H. Salamati, J.M. D. Coey, J. Appl. Phys. 110 (2011), 043905.
[18] A.M. Tishin, Y.I. Spichkin, The Magnetocaloric Effect and its Applications, Institute of Physics Publishing, Bristol and Philadelphia, 2003.
[19] K.A. GschneidnerJr, V.K. Pecharsky, A.O. Tsokol, Rep. Prog. Phys. 68 (2005) 1479.
[20] T. Samanta, I. Das, S. Banerjee, Appl. Phys. Lett. 91 (2007), 152506.
[21] T. Samanta, I. Das, S. Banerjee, Appl. Phys. Lett. 91 (2007), 082511.
[22] B.S. Nagaraja, A. Rao, P.D. Babu, G.S. Okram, Physica B 479 (2015) 10–20.
[23] A.A. Wagh, P.S. Anil Kumar, H.L.Bhatand S. Elizabeth, J. Phys.: Condens. Matter 22 (2010), 026005.
[24] A.A. Wagh, P.S.A. Kumar, S. Elizabeth, Mater. Res. Express 3 (2016), 106102.
[25] S.K. Giri, T.K. Nath, J. Appl. Phys. 113 (2013) 17D706.
[26] K. Das, S. Mandal, D. Mazumdar, P. Sen, I. Das, J. Magn. Magn. Mater. 501 (2020), 166421.
[27] R. Zhang, J. Magn. Magn. Mater. 428 (2017) 464–468.
[28] T S.K. Banerjee, Phys. Lett. 12 (1964) 16.
[29] W.J. Lu, X. Luo, C.Y. Hao, W.H. Song, Y.P. Sun, J. Appl. Phys. 104 (2008), 113908.
[30] A. Biswas, S. Chandra, M.H. Phan, H. Srikanth, J. Alloys Compd. 545 (2012) 157.